Letters in Applied NanoBioScience
Open-Access Journal (ISSN: 2284-6808)

Article
Volume 12, Issue 4, 2023, 115
https://doi.org/10.33263/LIANBS124.115

Graphene from Sugarcane Bagasse for Nonenzymatic Electrochemical Determination of Glucose

Jhuma Debbarma [1], Ranjit Debnath [1], Mitali Saha [1,*]

[1] Department of Chemistry, National Institute of Technology Agartala, Tripura-799046, India
* Correspondence: mitalichem71@gmail.com (M.S.)

Scopus Author ID 5779373600
Received: 4.04.2022; Accepted: 16.05.2022; Published: 18.09.2022

Abstract: Graphene prepared from sugarcane bagasse was utilized to fabricate an electrode for the electrochemical determination of glucose under non-enzymatic conditions. Sugarcane bagasse was pyrolyzed at relatively low temperatures to produce graphene, which was used as electrode material for glucose sensing using cyclic voltammetry (CV) and amperometry (AMP). The CV results demonstrated that the fabricated graphene electrode showed good linearity in the glucose concentration range of 50-900 mg/L with a sensitivity value of 10.352 $\mu AM^{-1}cm^{-2}$ and a detection limit of 1.13 µM at pH 5.2. The efficiency and selectivity of the electrode were evaluated by amperometry studies in three real samples, viz. apple juice, coco-cola, and honey, where the glucose concentration was found to be 1.88%, 4.2%, and 40.75%, respectively, compared with those available in the literature. Further, the electrode showed a rapid response of 6s and possessed stability of 87.5% of the initial value up to 15 days. Thus, it was suggested that the synthesized graphene from bagasse fibers can act as an efficient electrode material for the electrochemical determination of glucose. It can also be explored for other sensing applications under non-enzymatic conditions.

Keywords: graphene; β –D glucose; cyclic voltammetry; amperometry; real samples analysis.

1. Introduction

In current ages, graphene and its derivatives have been paid considerable attention to the development of economical yet rapid glucose sensors [1-9]. Generally, electrochemical sensing has a great deal of interest in the electrochemical oxidation of glucose because this method has a low power requirement and high sensitivity [10-23]. Over a decade, the construction of glucose sensors mostly relies on graphene oxide (GO) or reduced graphene oxide (rGO). However, it is now well established that sensors or biosensors fabricated from pristine graphene showed high sensitivity, selectivity, stability, and reproducibility as compared to GO/rGO [24-26]. In this aspect, methods to prepare pristine graphene in bulk need to be explored for developing sensors. It is further understood that enzyme-based glucose sensors are costly, unstable, and severely suffer from changes in pH, temperature, etc., so designing non-enzymatic glucose sensing platforms is highly demanded nowadays. Because of all these observations, the inexpensive pristine graphene-based non-enzymatic sensor is yet to be explored.

As reported earlier, sugarcane bagasse was successfully utilized to prepare graphene and its derivatives in bulk amounts at relatively low temperatures [27-29]. To ensure the selectivity and sensitivity toward detection of glucose, graphene synthesized from the bagasse

fibers was utilized to fabricate electrodes for the cyclic voltammetry and amperometry studies towards the determination of glucose under non-enzymatic conditions. It was fascinating to report that this graphene-modified electrode showed good stability, repeatability, and sensitivity with a low detection limit of glucose in real samples. The amperometric detection of glucose was also performed to measure the concentration of real samples (scheme 1).

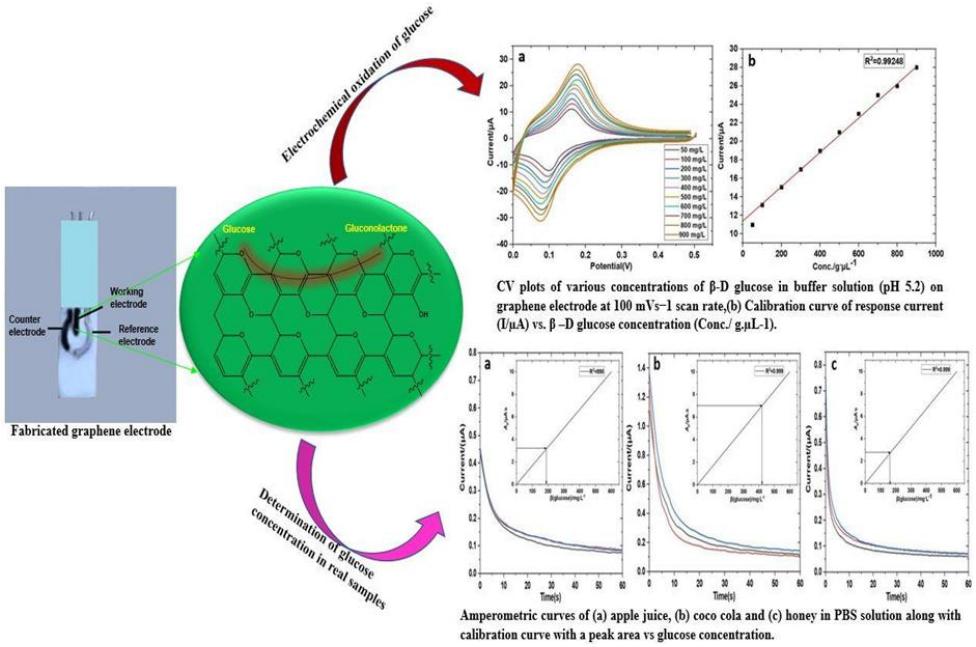

Scheme 1. Graphical abstract of electrochemical oxidation of glucose at fabricated graphene electrode.

2. Materials and Methods

D-(+)-glucose anhydrous ($C_6H_{12}O_6$), potassium dihydrogen phosphate (KH_2PO_4), sodium hydrogen phosphate (Na2HPO4), and potassium chloride (KCl) were purchased from Sigma. Silver wires of 99.999% purity were purchased from Sigma and used to fabricate the graphene electrode. Potassium ferricyanide ($K_3[Fe(CN)_6]$), polystyrene, and chloroform were purchased from merk. Electrochemical studies were performed using a mini 910 PSTAT (Ω Metrohm), where a screen-printed CNT electrode was used as a standard electrode. 100 ml buffer solution was prepared by mixing 0.816 g KH_2PO_4, 0.099 g Na_2HPO_4, and 0.745 g KCl in 100 ml of deionized water and kept at 4 ^oC before use. The stock solution of β-D glucose in 100 ml was prepared by dissolving 1 g β-D glucose in buffer solution (pH 5.2) with gentle stirring. The glucose solutions of different concentrations were prepared by diluting the stock solution in a buffer solution.

2.1. Fabrication of electrode using graphene from sugarcane bagasse.

As mentioned in our earlier work, graphene was prepared from sugarcane bagasse [28]. An electrode having dimensions of 3.5 cm x 1.0 cm x 0.5 cm (length x width x height) was fabricated on an insulating Teflon material containing three silver wires. A dense solution of graphene powder and polystyrene was prepared in chloroform and deposited on the Teflon surface, which acted as a working electrode and the counter electrode. Silver wires prepared the reference electrode and electric contacts.

2.2. Standardization of screen-printed carbon nanotubes (std-CNT) electrode.

A standard solution of hexacyanoferrate (III) of 0.1 mol/L was prepared, and standardization was carried out using a screen-printed std-CNT electrode in the presence of ammonium acetate buffer (pH 4.6) by cyclic voltammetry at a scan rate of 100 mVs^{-1}. The ratio of cathodic to anodic current was calculated.

2.3. Non-enzymatic electrochemical detection of glucose using graphene electrode.

For non-enzymatic detection of β–D glucose, cyclic voltammetry (CV) and amperometry studies were performed at fabricated graphene electrodes. The scan rate and time interval effect were investigated by CV using 100 mg/L of glucose solution in phosphate buffer (pH = 5.2). Further, different concentrations of glucose solutions (50-900 mg/L) were prepared in phosphate buffer to study the fabricated graphene electrode's linearity, detection limit, and sensitivity. The amperometric measurements were performed in the fabricated graphene electrode using real samples, viz., apple juice, coco-cola, and honey, to determine the concentration of glucose in each sample. The sample solutions of apple juice and coco-cola were prepared in phosphate buffer (0.1:10 ratio).

Similarly, the honey sample solution was prepared in the phosphate buffer, maintaining the same ratio. The amperometric measurements of the real samples were carried out, and the current response was observed within the 60s. The determination of various analytical parameters, viz. concentration, repeatability, and stability of the fabricated graphene electrode, were carried out. The calibration curves were plotted to determine glucose concentrations in all the real samples.

3. Results and Discussion

The fabricated graphene electrode has presented in Figure 1a. CV study was performed with graphene electrode using 0.1 mol/L $[K_3Fe(CN)_6]$ in ammonium acetate buffer solution and was compared with the screen-printed standard (std-CNT) electrode at the scan rate of 100 mVs^{-1}. Figure1b showed that the ratio of the cathodic to the anodic current was nearly 1 in both the cases and the peak potential was found to be nearly 0.60 V. This result was in good agreement with the Nernst equation for one electron system. The electrochemical response of the graphene electrode was comparable to std-CNT, which suggested that the graphene electrode can be used for electrochemical studies like the std-CNT electrode.

3.1. Effect of scan rate and time interval of glucose at graphene electrode.

The effect of the scan rate on the performance of the fabricated graphene electrode was investigated by CV using 100 mg/L glucose solutions at a scan rate of 50-200 mVs^{-1}, as shown in Figure 2a. The graphene electrode was used as both the working electrode and counter electrode, while the silver wire acted as a reference electrode. Figure 2a suggested that when the current vs scan rate was plotted within the range of 50-200 mVs^{-1}, a linear relationship was observed between the peak intensity I(μA) and the scan rate(mVs^{-1}) via the linear regression equation I(μA) = 3.4774 + 0.823 (mVs^{-1}) where, the regression coefficient (R^2) was found to be 0.99826 along with standard deviation (SD) = 0.4743, N = 4 (Figure 2a(a_1)). It indicated that glucose oxidation at the graphene electrode surface was adsorption-controlled. A plot of the logarithm of peak current vs. logarithm of scan rate also gave a straight line with a slope of

0.961 (Figure 2a(a_2)), which is found to be closed to the theoretical value of 1 for a purely adsorption-controlled process [30,31]. The linear regression equation was observed as log I/µA = 0.8725+0.961 log m/mVs^{-1} with the value of R^2 = 0.96950, standard deviation (SD) = 0.0726, N = 4.

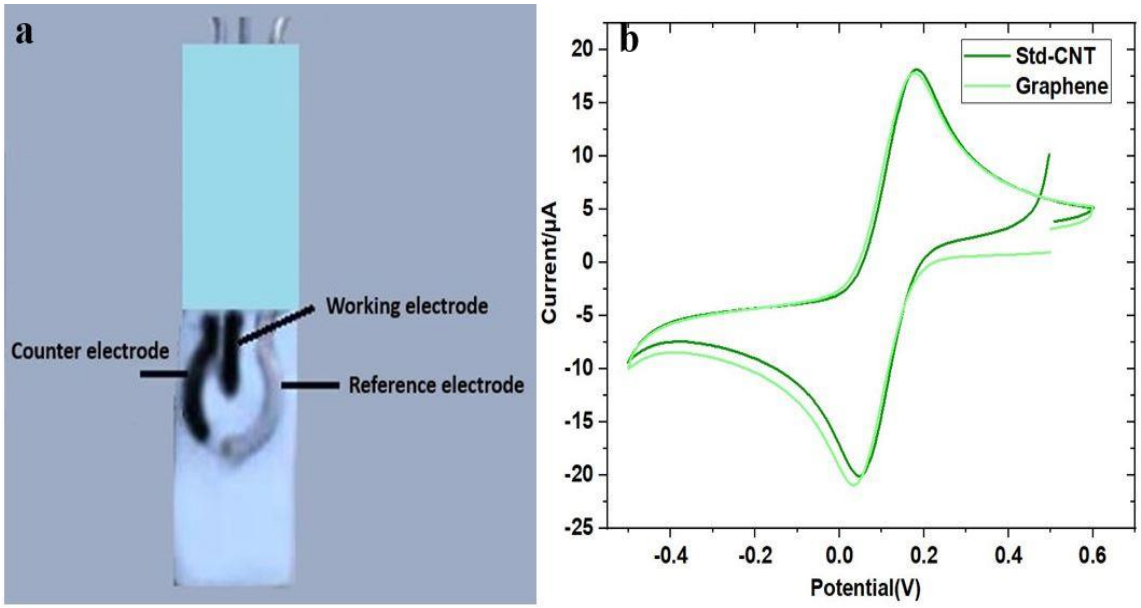

Figure 1. (a) Image of fabricated graphene electrode towards the detection of glucose under non-enzymatic conditions, (b) CV plots of 0.1 mol/L [$K_3Fe(CN)_6$] in ammonium acetate buffer solution at 100 mVs−1 on the screen-printed std-CNT and prepared graphene electrode.

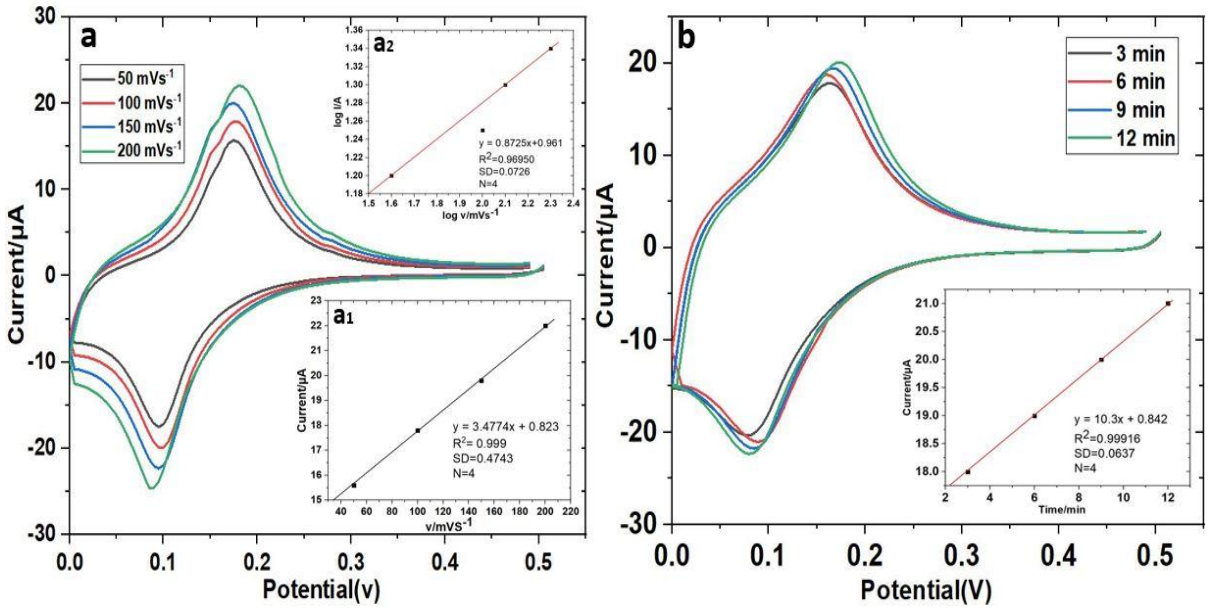

Figure 2. (a) CV plots of β-D glucose (100 mg/L) in phosphate buffer (pH 5.2) solution at various scan rates (50,100,150, and 200 mVs^{-1}) on graphene electrode with inset (a_1) the plot of peak current (I/µA) vs. scan rate (ν/mVs^{-1}), (a_2) the plot of the logarithm of peak current vs. logarithm of scan rate. (b) CV plots of β-D glucose (100 mg/L) in phosphate buffer solution at various time intervals (3,6,9 and 12 min) at 100 mVs^{-1} scan rate on graphene electrode at pH 5.2 with inset the plot of peak current (I/µA) vs. time interval (t/min).

Figure 2b shows the effect of time interval (3-12 min) on peak current at graphene electrode (100 mVs^{-1}). The calibration plot showed good linearity between the current and the time interval, and the linear regression equation was found to be I/µA = 10.3+ 0.842 t/min (R^2 = 0.99916). It was observed that when the time interval was extended up to 20 min, it resulted in a breakdown of the direct proportionality between peak current and time. This might be

because, with the increase in time, the peak current gradually increased, but after 12 min, the peak current reached the maximum value and became stable.

3.2. Linearity, detection limit, and sensitivity of the graphene electrode.

To determine the quantitative analysis of β–D glucose at fabricated graphene electrode, CV was employed with various glucose concentrations (50-900 mg/L) in PBS solution (pH 5.2) at a scan rate of 100 mVs^{-1} as presented in Figure 3a. It was observed that the peak current increased linearly with the increasing concentration of glucose (Figure 3a). Figure 3b shows that the electrode showed good linearity in the glucose concentration range of 50-900 mg/L. The linear regression equation for 50-900 mg/L of glucose concentrations was found to be, I/µA = 10.984 + 0.792 mg/L, where slope was 0.792. The observed correlation coefficient (R2) value was 0.99248 for β –D glucose.

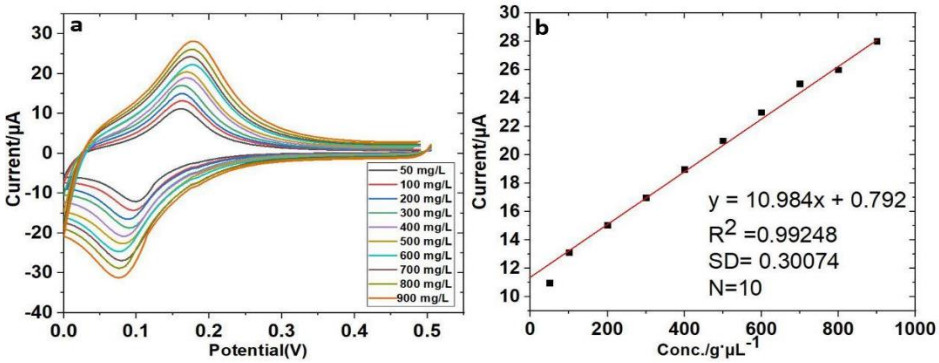

Figure 3. (a) CV plots of β -D glucose (50 –900 mg/L) in buffer solution (pH 5.2) on graphene electrode at 100 mVs−1 scan rate and (b) Calibration curve of response current (I/µA) vs. β –D glucose concentration (conc./g.µL-1).

The active surface area of the graphene electrode was calculated using Randles–Sevcik equation.

$$IP = (2.69 \times 10^5)n^{3/2}AD^{1/2}C\nu^{1/2}$$

where ν is the scan rate (mVs^{-1}), C is the concentration of the redox probe molecule (mg/L), D is the diffusion coefficient (cm^2s^{-1}), A is the electroactive surface area (cm^2) of the electrode, and n is the number of electrons participating in the redox reaction. It is well established that the diffusion coefficient depends on the electrode's scan rate, concentration, and working area 18,19. The electroactive surface area of the graphene electrode was calculated and found to be 0.0765 cm^2, where C = 0.1 M, D = 7.57×10^{-7} cm^2/s for $[Fe(CN)6]^{3-/4-}$ system. The sensitivity was calculated as 10.352 $\mu A \mu M^{-1} cm^{-2}$ from the current versus concentration plot via slope/active surface area (Figure 3b). The limit of detection (LOD) and limit of quantification (LOQ) were calculated using the formulas LOD = 3s/m, LOQ = 10 s/m, which were found to be 1.13 µM and 3.7 µM, respectively. s and m being the standard deviation of the peak currents and slope of the calibration curve were found to be 0.30074 and 0.792, respectively.

3.3. Amperometric determination of glucose in real samples at graphene electrode.

To estimate the accuracy of the fabricated graphene electrode in the determination of glucose concentration, amperometric measurements were carried out in three real samples, namely apple juice, coco-cola, and honey. 100 mg/L of real samples were prepared, and amperometric responses of graphene electrode were evaluated. It is clear from Figure 4(a-c)

that a clear and rapid response of graphene electrode was observed in 60 s and a linear relationship existed between the glucose concentration (mg/L) and the peak area (Ap/µA.s) in each case.

The concentration of glucose in all the samples was calculated using the volume correction method, i.e., $C_{sample} = C_{sample\ solution}\ V_{total}/V_{sample}$, where, $C_{sample\ solution}$ is the concentration in the sample solution, V_{total} is the total volume of the sample solution, V_{sample} is the volume of sample in the sample solution and C_{sample} is the concentration of glucose in a sample solution. Table 1 displays the glucose concentration of all three samples determined using a fabricated graphene electrode. The experimental results were compared with those available in the literature [32-34]. The obtained results confirmed that the synthesized graphene using bagasse fibers might be utilized as electrode materials for sensing applications.

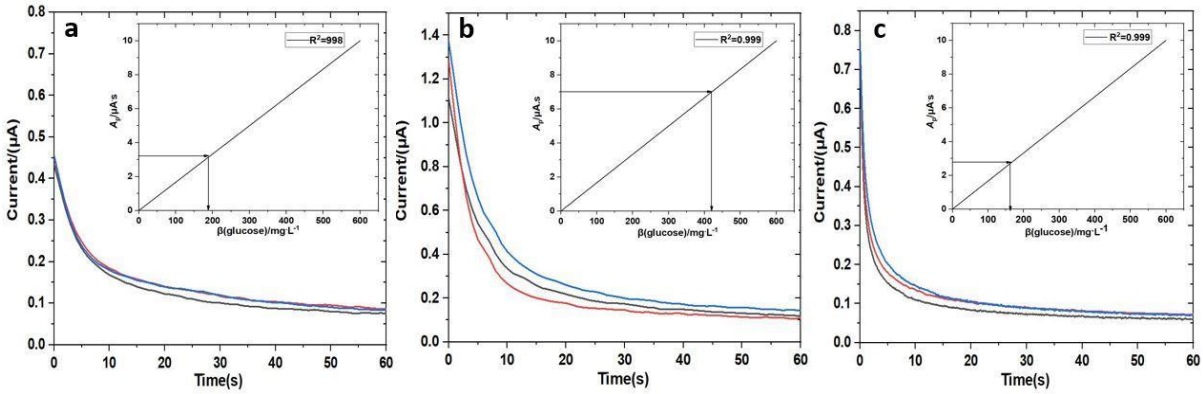

Figure 4. Amperometric curves of (a) apple juice, (b) coco-cola, and (c) honey in a PBS solution along with a calibration curve with a peak area vs. glucose concentration.

Table 1. Determination of glucose concentration in real samples at graphene electrode.

Sample	Reported glucose concentration(%)	Determination of glucose concentration(%)	RSD(%)
Apple juice	2.5	1.88	5.517
Coco cola	5	4.2	12.546
Honey	34.9	40.75	4.456

3.4. Repeatability and stability of fabricated graphene electrode.

The repeatability of the graphene electrode was studied by measuring the current responses of honey using 100 mg/L solutions in PBS (pH 5.2), as presented in Figure 5(a). The experiments were carried out 4 times using the same concentration of the honey solution.

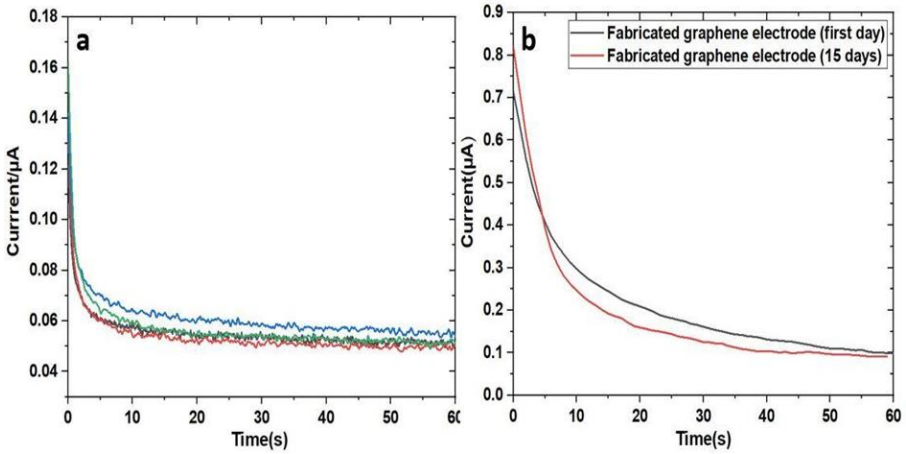

Figure 5. (a) Repeatability and (b) stability of fabricated graphene electrode.

The current response measurements showed a relative standard deviation (RSD) of 7.5%, signifying that the graphene electrode presented acceptable repeatability and reusability. The stability of the proposed graphene electrode was observed as 87.5% of the initial value within 15 days (Figure 5(b)).

4. Conclusions

This paper used graphene prepared from sugarcane bagasse to fabricate electrodes for glucose sensing under non-enzymatic conditions. The results indicated that the fabricated electrode showed good linearity in the glucose concentration range of 50-900 mg/L, showing a sensitivity value of 10.352 $\mu AM^{-1}cm^{-2}$ and a detection limit of 1.13 µM at pH 5.2. To ensure the selectivity and suitability, the graphene electrode was also utilized to determine the glucose concentration in three real samples, apple juice, coco-cola, and honey, where the concentrations of glucose were found to be comparable with the literature value. Moreover, the electrode showed a rapid response of 6 s with excellent stability of 87.5% of the initial value, up to a period of 15 days. It confirmed that this low-cost fabricated graphene electrode with enhanced electrocatalytic performances might be explored for other sensing applications under non-enzymatic conditions.

Funding

This research received no external funding.

Acknowledgments

The authors are thankful to the Department of Chemistry, NIT Agartala.

Conflicts of Interest

The authors declare no conflict of interest.

References

1. Fu, X.; Chen, Z.; Shen, S.; Xu, L.; Luo, Z. Highly sensitive non-enzymatic glucose sensor based on reduced graphene oxide/ultrasmall Pt nanowire nanocomposites. *Int. J. Electrochem. Sci.* **2018**, *13*, 4817-4826, https://doi.org/10.20964/2018.05.46.
2. Ayranci, R.; Demirkan, B.; Sen, B.; Şavk, A.; Ak, M.; Şen, F. Use of the monodisperse Pt/Ni@ rGO nanocomposite synthesized by ultrasonic hydroxide assisted reduction method in electrochemical non-enzymatic glucose detection. *Mater Sci Eng C* **2019**, *99*, 951-956, https://doi.org/10.1016/j.msec.2019.02.040.
3. Darvishi, S.; Souissi, M.; Kharaziha, M.; Karimzadeh, F.; Sahara, R.; Ahadian, S. Gelatin methacryloyl hydrogel for glucose biosensing using Ni nanoparticles-reduced graphene oxide: an experimental and modeling study. *Electrochim. Acta* **2018**, *261*, 275-283, https://doi.org/10.1016/j.electacta.2017.12.126.
4. Heidari, H.; Habibi, E. Amperometric enzyme-free glucose sensor based on the use of a reduced graphene oxide paste electrode modified with electrodeposited cobalt oxide nanoparticles. *Microchim. Acta* **2016**, *183*, 2259-2266, https://doi.org/10.1007/s00604-016-1862-z.
5. Chung, J.S.; Hur, S.H. A highly sensitive enzyme-free glucose sensor based on Co3O4 nanoflowers and 3D graphene oxide hydrogel fabricated via hydrothermal synthesis. *Sens. Actuators B Chem* **2016**, *223*, 76-82, https://doi.org/10.1016/j.snb.2015.09.009.
6. Hui, N.; Wang, J. Electrodeposited honeycomb-like cobalt nanostructures on graphene oxide doped polypyrrole nanocomposite for high performance enzymeless glucose sensing. *J. Electroanal. Chem* **2017**, *798*, 9-16, https://doi.org/10.1016/j.jelechem.2017.05.021.
7. Meng, A.; Sheng, L.; Zhao, K.; Li, Z. A controllable honeycomb-like amorphous cobalt sulfide architecture directly grown on the reduced graphene oxide–poly (3, 4-ethylenedioxythiophene) composite through

electrodeposition for non-enzyme glucose sensing. *J Mater Chem B.* **2017**, *5*, 8934-8943, https://doi.org/10.1039/C7TB02482G.
8. Samoson, K.; Thavarungkul, P.; Kanatharana, P.; Limbut, W. A non-enzymatic glucose sensor based on the excellent dispersion of a graphene oxide-poly (acrylic acid)-palladium nanoparticle-modified screen-printed carbon electrode. *J. Electrochem. Soc* **2019**, *166*, https://doi.org/10.1149/2.1381912jes.
9. Wang, M.; Ma, J.; Chang, Q.; Fan, X.; Zhang, G.; Zhang, F.; Li, Y. Fabrication of a novel ZnO–CoO/rGO nanocomposite for non-enzymatic detection of glucose and hydrogen peroxide. *Ceram. Int.* **2018**, *44*, 5250-5256, https://doi.org/10.1016/j.ceramint.2017.12.136.
10. Balayan, S.; Chauhan, N.; Chandra, R.; Jain, U. Electrochemical Based C-Reactive Protein (CRP) Sensing Through Molecularly Imprinted Polymer (MIP) Pore Structure Coupled with Bi-Metallic TunedScreen-Printed Electrode. *Biointerface Res. Appl. Chem.* **2022**, *12*, 7697-7714, https://doi.org/10.33263/BRIAC126.76977714.
11. Aruna, P.; Prasad, P.R.; Sadhya, P.; Seshagiri, N.V.S.S. Biosynthesis of α-Fe2O3-CdO Nanocomposites for Electrochemical Detection of Chloridazon Herbicide. *Biointerface Res. Appl. Chem.* **2022**, *12*, 5772–5784, https://doi.org/10.33263/BRIAC125.57725784.
12. Zahan, M.; Podder, J. Synthesis and Characterizations of Cu Doped Co3O4 Nanostructured Thin Films Using Spray Pyrolysis for Glucose Sensor Applications. *Biointerface Res. Appl. Chem.* **2022**, *12*, 6321–6335, https://doi.org/10.33263/BRIAC125.63216335.
13. Ononiwu, N.H.; Ozoegwu, C.G.; Madushele, N.; Akinribide, O.J.; Akinlabi, E.T. Mechanical Properties, Tribology and Electrochemical Studies of Al/Fly Ash/Eggshell Aluminium Matrix Composite. *Biointerface Res. Appl. Chem*. **2022**, *12*, 4900–4919, https://doi.org/10.33263/BRIAC124.49004919.
14. Arham, Z.; Kurniawan, K.; Ismaun, I. Synthesis of TiO2 Photoelectrode Nanostructures for Sensing and Removing Textile Compounds Rhodamine B. *Biointerface Res. Appl. Chem*. **2022**, *12*, 5479–5485, https://doi.org/10.33263/BRIAC124.54795485.
15. Izham, N.Z.M.; Yusoff, H.M.; Binti Asari, A.; Haq, I.U. Potential Recognition Layer in Electrochemical Sensor: A Comparative Characterization of p-Cyano Schiff Base Compounds. *Biointerface Res. Appl. Chem.* **2022**, *12*, 1803–1813, https://doi.org/10.33263/BRIAC122.18031813.
16. Tkach, V.V.; Kushnir, M.V.; Kopiika, V.V.; Luganska, O.V.; Omelianchyk, L.O.; Gencheva, V.I.; Palytsia, Y.V. Theoretical description for the electrochemical determination and retention of heavy metals over the overoxidized polypyrrole by complex formation. *Biointerface Res. Appl. Chem*. **2022**, *12*, 1273-1278, https://doi.org/10.33263/BRIAC121.12731278.
17. Sharma, V.; Vashistha, V.K.; Das, D.K. Biological and electrochemical studies of macrocyclic complexes of iron and cobalt. *Biointerface Res Appl Chem*. **2021**, *11*, 7393-7399, https://doi.org/10.33263/BRIAC111.73937399.
18. Kornet, M.M.; Brazhko, O.A.; Zavhorodniy, M.P.; Tkach, V.V.; Kruglyak, O.S.; Ivanushko, Y.G.; Yagodynets, P.I. Electrochemical Determination of Antioxidant Activity of New 4-Thiosubstituted Quinoline Derivatives with Potential Radioprotecting Properties. *Biointerface Res Appl Chem*. **2021**, *11*, 9148–9156, https://doi.org/10.33263/BRIAC112.91489156.
19. Tkach, V.V.; Kushnir, M.V.; de Oliveira, S.C.; Ivanushko, J.G.; Velyka, A.V.; Molodianu, A.F.; Bredikhina, Y.L. Theoretical description for anti-COVID-19 drug Remdesivir electrochemical determination, assisted by squaraine Dye–Ag2O2 composite. *Biointerface Res Appl Chem*. **2021**, *11*, 9201-9208, https://doi.org/10.33263/BRIAC112.92019208.
20. Ramakrishna, M. G.; Girigoswami, A.; Chakraborty, S.; Girigoswami, K. Bisphenol A-An Overview on its Effect on Health and Environment. *Biointerface Res Appl Chem*. **2022**, *12*, 105-119, https://doi.org/10.33263/BRIAC121.105119.
21. Kormosh, Z.O.; dos Reis, L.V. Theoretical Description for Chlorantraniliprole Electrochemical Determination, Assisted by Squaraine Dye Nano Ag2O2 Composite. *Biointerface Res Appl Chem*. **2021**, *11*, 9278–9284, https://doi.org/10.33263/BRIAC112.92789284.
22. Tkach, V.V.; Kushnir, M.V.; Kopiika, V.V.; Luganska, O.V.; Kormosh, Z.O.; Nazymok, Y.V.; Yagodynets, P.I. Theoretical Description for Orellanine Electrochemical Determination and Electropolymerization in the Presence of Hydroquinones, Assisted by CuS Nanoparticles. *Biointerface Res Appl Chem*. **2021**, *11*, 10607–10613, https://doi.org/10.33263/BRIAC113.1060710613.
23. Gopinath, S.K.; Pari, M.; Rudrannagari, A.; Kattebasaveshwara, I.B.; Halappa, S.K. Synthesis, Characterization and Electrochemical Sensor Based Upon Novel Schiff Base Metal Complexes Derived from the Non-Steroidal Anti-inflammatory Drug, Flufenamic Acid for the Determination of Uric acid and their Biological Applications. *Biointerface Res Appl Chem*. **2021**, *11*, 11390–11403, https://doi.org/10.33263/BRIAC114.1139011403.
24. Miao, F.; Wu, W.; Miao, R.; Cong, W.; Zang, Y.; Tao, B. Graphene/nano-ZnO hybrid materials modify Ni-foam for high-performance electrochemical glucose sensors. *Ionics* **2018**, *24*, 4005-4014, https://doi.org/10.1007/s11581-018-2539-x.
25. Wu, H.; Yu, Y.; Gao, W.; Gao, A.; Qasim, A.M.; Zhang, F.; Chu, P.K. Nickel plasma modification of graphene for high-performance non-enzymatic glucose sensing. *Sens. Actuators B Chem*. **2017**, *251*, 842-850, https://doi.org/10.1016/j.snb.2017.05.128.

26. Yang, J.; Lin, Q.; Yin, W.; Jiang, T.; Zhao, D.; Jiang, L. A novel non-enzymatic glucose sensor based on functionalized PDDA-graphene/CuO nanocomposites. *Sens. Actuators B Chem*. **2017**, *253*, 1087-1095, https://doi.org/10.1016/j.snb.2017.07.008.
27. Debbarma, J.; Naik, M.J.P.; Saha, M. From agrowaste to graphene nanosheets: chemistry and synthesis. *Fuller Nanotub Car N*. **2019**, *27*, 482-485, https://doi.org/10.1080/1536383X.2019.1601086.
28. Debbarma, J.; Mandal, P.; Saha, M. Chemistry and mechanism of one-step formation of graphene from agrowaste. *Lett. Appl. Nanosci*. **2020**, *9*, 1389-1394, https://doi.org/10.33263/LIANBS93.13891394.
29. Debbarma, J.; Banik, S.; Saha, M. Valorization of Sugarcane Bagasse to Sulfur Containing Graphene: Chemistry and Mechanism. *J. Nat. Fibers* **2021**, *18*, 1-6, https://doi.org/10.1080/15440478.2021.1993407.
30. Gosser, D.K. *Cyclic voltammetry: simulation and analysis of reaction mechanisms*. New York: VCH. **1993**; pp. 43, https://doi.org/10.1002/elan.1140070324.
31. Bard, A.J.; Faulkner, L.R. Fundamentals and applications. *Electrochem. Methods*. **2001**, *2*, 580-632.
32. Shi, R.; Stein, K.; Schwedt, G. Spectrophotometric determination of glucose in foods by flow injection analysis with an immobilized glucose oxidase reactor. *Zeitschrift für Lebensmitteluntersuchung und-Forschung A* **1997**, *204*, 99-102, https://doi.org/10.1007/s002170050044.
33. Meurman, J.H.; Rytömaa, I.; Kari, K.; Laakso, T.; Murtomaa, H. Salivary pH and glucose after consuming various beverages, including sugar-containing drinks. *Caries Res.* **1987**, *21*, 353-359, https://doi.org/10.1159/000261039.
34. Wahdan, H.A.L. Causes of the antimicrobial activity of honey. *Infection* **1998**, *26*, 26-31, https://doi.org/10.1007/BF02768748.